March 2018

Direct Print Additive Manufacturing of Optical Fiber Interconnects

Roger B. Tipton
University of South Florida, rbtipton@hotmail.com

Direct Print Additive Manufacturing of Optical Fiber Interconnects

by

Roger B. Tipton

A thesis submitted in partial fulfillment
of the requirements for the degree of
Master of Science in Materials Science and Engineering
Department of Chemical and Biomedical Engineering
College of Engineering
University of South Florida

Co-Major Professor: Venkat Bhethanabotla, Ph.D.
Co-Major Professor: Thomas Weller, Ph.D.
Jing Wang, Ph.D.

Date of Approval:
March 12, 2018

Keywords: 3D Printing, 3D Printed Optical Fiber, DPAM, 3D printed optics

DEDICATION

I would like to dedicate this work to my wife, Rachel, and our two boys Henry and Jack who have supported my education and this research and are the reason that I work this hard.

ACKNOWLEDGMENTS

I would like to thank my co-advisers, Dr. Thomas Weller and Dr. Venkat Bhethanabotla for the opportunity to engage in this research.

Thank you to my entire committee of Dr. Thomas Weller, Dr. Venkat Bhethanabotla and Dr. Jing Wang for their time and effort in contributing to my thesis.

To the research teams in Dr. Weller and Dr. Bhethanabotla's labs that provided support to this research, your help was very much appreciated.

I would like to thank Christopher Stevens in Dr. Denis Karaiskaj's Laser Spectroscopy Lab who trained me in the design and fabrication of the optical test equipment and procedures to use them for this research.

I spent a lot of hours working in the USF Nanotechnology Research & Education Center and would like to say thank you to their team for their support.

In addition to the team at the University of South Florida, I would like to recognize Eduardo Rojas, Ph. D from the Embry-Riddle Aeronautical University who provided his guidance and knowledge and helped to make this research possible.

TABLE OF CONTENTS

LIST OF TABLES

LIST OF FIGURES

ABSTRACT

High performance communications, sensing and computing systems are growing exponentially as modern life continues to rely more and more on technology. One of the factors that are currently limiting computing and transmission speeds are copper wire interconnects between devices. Optical fiber interconnects would greatly increase the speed of today's electronic devices. In this study it has been demonstrated that by using a new Direct Print Additive Manufacturing (DPAM) process of Fused Deposition Modeling (FDM) of plastic and micro-dispensing of pastes and inks, we can 3D print single and multi-mode optical fibers in a controlled manner such that compact, 3-dimensional optical interconnects can be printed along non-lineal paths.

We are FDM printing the core materials from a plastic PMMA material. We are dispensing a urethane optical adhesive as the core material. These materials are available in many different refractive indices. During numerical simulations of these fibers, we were able to show through manipulation of the refractive indices of the core and cladding that we can also improve the bend performance of our fibers. As a result, they can perform better as an interconnect in tight routings between components as long as the interconnect fiber distances remain less than 1 meter.

Fibers have been fabricated with diameters between 77 and 17 μm across an air gap with a surface roughness of less than 450 nm and cladded and tested with transmission rates of about 46%. 12 μm fibers have successfully been fabricated on a cladded surface as a proof of concept to test the small diameter and 3D shaping capability of this process.

CHAPTER 1:

INTRODUCTION

Integrated photonics have many compelling advantages for computing and communications applications, including high-speed and extremely wide bandwidth operations. There remain challenging barriers to widespread implementation, however, two of the most significant obstacles are low cost fiber packaging and electronic-photonic integration. [1] Today's systems are typically hybrid assemblies of packaged photonic devices (integrated circuits) that are interconnected with separate fibers and wire harnesses. Printed circuit boards often serve to route electrical signals and power, and in some cases, have runs of optical fibers. In general, these are complex systems with a mix of technologies and the supporting manufacturing infrastructure is expansive.

Recent developments in additive manufacturing have motivated new research in optical devices. These developments can be broadly categorized into sintered glasses, plastic inks and commercial fiber integration. Glasses can be additively manufactured using a dispensed 20 wt% silica in a tetraglyme carrier through a 500 μm nozzle. This ink is then processed for up to 113 hours to slowly evaporate the solvents and organics, followed by a high temperature sinter at 1,500°C. The long processing time is used to prevent residual stresses from forming and causing defects that lead to issues with transmission and mechanical properties.[2, 3] Glasses can also be printed using a stereolithography process using SiO2 nanoparticles that are once again de-binded and sintered to form a solid. This layered process creates a rough surface that cannot be used for

light transmission.[4] Another glass technology is a fused deposition modeling of a molten soda lime glass that has been heated to around 1,000°C and forced through an extruder nozzle. At this point, the surface finish of the glass is not smooth enough to be used for optical transmission. A variation of this method is where a filament of glass is melted with a laser and deposited on a surface. Once again, the surface finish with this method is insufficient for optical transmission.[5]

There are also innovations based on using plastic inks to create optical waveguides that are being pursued in the IC and MEMS industries. Inkjet printing using InkOrmo, InkEpo and Microresist Technology inks are being used to create "soft" rectangles and a round light is then injected through the rectangular waveguide. This is a relatively new approach, and to date publications have focused primarily on process versus performance. Initial prototype development has focused mainly on IC applications.[6]

The third major additive manufacturing technology centers around using commercial optical technology and fibers to create physically large optical data transmission systems. The IBM Optochip is an example of applying existing technology to optical transmission where VSCEL emitters and receivers are embedded in a chip and are connected through lenses to standard optical fibers. Data transmission rates of up to 64 Gbps have been shown in the lab with this technology. The technology has been commercialized in an 8 Gbps supercomputing application. The drawbacks to this system include the large size of the connectors and fibers, and the implementation cost. Costs are currently over $0.50 per Gbps of transmission and interconnect densities are above 100 Gbps per cm2. The approach is considered to be most appropriate in applications where cost and size are not the major drivers.[7, 8]

The AM technique that will be explored in this work is direct print additive manufacturing (DPAM). This is a hybrid additive manufacturing method that combines fused deposition modeling (FDM) for thermoplastic deposition, with micro-dispensing/ink-jetting for inks, adhesives and pastes (conductive, resistive, insulating, etc.). The DPAM process is well explored for other applications including paste morphology and high frequency performance pulsed laser processing of micro-dispensed pastes, mm-wave attenuation of FDM waveguides, and processes for thermoplastic-ceramic composite FDM filaments.

The proposed DPAM approach provides a solution that is capable of straddling the integrated circuit and connectorized packaging length scales. The printing platform has micron-level positioning accuracy and repeatability, pico-liter control of micro-dispensing through nozzles down to 10-micron diameter, and minimum-layer thickness of ~25 microns for FDM-deposited thermoplastics. Aerosol-jet and inkjet print heads can be attached to the system to enable deposition of sub-micron thickness conductors. The build volume is 30 x 15 x 15 cm^3 on the existing USF system, and significantly larger platforms are possible. Finally, the baseplate and maximum temperature experienced by the components during printing is typically about 100° C once the materials leave the extrusion nozzle; this facilitates printing directly to and embedding packaged and bare die ICs.

In order to bring this versatile digital manufacturing capability to bear on a high performance multispectral interconnect fabrication, a series of technical advances are needed. High transmission capability for the optical fiber requires tight control over several DPAM parameters that influence surface roughness, fiber diameter, and achievable bend radius.

1.1 Electrical Interconnects

Signal attenuation is one of the largest issues of electrical interconnects due to resistance of the conductor and electric loss. These issues can be magnified at higher frequencies. Complex systems can be created to account for this with equalization and amplification up to the physical noise limitations.

One way to improve the performance of a conductor is to increase its cross-sectional area, which reduces it resistance. The downside to this is that we increase the cost of the conductor and increase the physical size requirements of the conduct which can limit the applications for this solution.

If size constraints are important, simply scaling the conductor down does not increase the bit rate capacity of the line due to the resistance x capacitance time constant of the wire which sets the shortest pulse that could readily be sent on the line. This makes the information carrying capacity of the electrical conductor independent of the size of the line. To better explain this, there are two types of electrical wiring, resistive capacitive (RC) and inductive capacitive (LC). Whether a line is RC or LC at a given frequency is primarily determined by its cross-sectional size which determines whether resistive (limited by the bulk resistance of the metal) or inductive (crowding of the current towards the surface of the wire) impedance dominates at a given frequency. At the gigahertz frequencies of modern electronics, interconnected lines on chips are RC controlled and off chip is LC controlled. [9, 10]

The capacity of electrical lines from such resistive limits can be written approximately as:

$$B \leq B_0 \frac{A}{L^2} \tag{1}$$

where A is the cross-sectional area of the conductor, L is the length of the conductor, B_0 is a constant and is approximately 10^{16} for RC-limited lines on a chip and approximately 10^{17} for inductive capacitive lines with resistive loss for off-chip equalized RLC lines.

Another important consideration is that the overall energy consumption of computer systems is becoming ecologically significant and optical interconnects can help reduce this power consumption. The three main core operations of a computer system are logic switching, memory and interconnects where the interconnects amount for the highest energy dissipation.[10] Energy loss for optical interconnect systems are inherently less as no heat is generated by the fiber during operation as there is a metal conductor.

1.2 Optical Interconnects

When we look to other options that can solve the problem of limited high frequency data transmission, optics is arguably the best option moving forward. In optical interconnects, the very low loss and dispersion of optical fiber allows for much higher rate of information transmission. At short distances, optics can help in interconnect density, interconnect power, improve signal integrity and timing.[11-13] The current issue with optical interconnects revolves around some basic issues. We must determine how to route optics through tight spaces without high losses due to scattering. We must also determine how to connect optics to light generating sources. And finally, we must determine how to integrate single mode fibers into tightly packaged interconnects to increase transmission rates.

1.3 Looking Forward at Our New Technology

Moving optical interconnects down to electronic devices requires the development of several new technologies. Vertical-cavity-surface-emitting lasers were the first technology to be

created that can emit tiny semiconducting light waves. The next technology required is tiny optical fibers that can easily be "shaped" through small spaces. Conventional silica optical fiber is one solution, but they are difficult for assembly at this size and can scatter light significantly if subjected to tight bend radii. Silica fibers also use very small delta n values and typically use an infrared wavelength of light. Extruded plastic optical fibers have been developed and they are used primary as large connectors outside the computer connecting servers together or to connect servers to network devices.

A new direct manufactured plastic optical interconnect has been developed that overcomes these issues with standard silica optical fibers and standard plastic optical fibers. Using a micro-dispensed UV curable urethane as a cladding, we created a surface where we used Fused Deposition Modeling (FDM), an additive manufacturing process, to place a core of polymethyl methacrylate (PPMA) onto the cladding material. We applied more micro-dispensed UV curable urethane to complete the cladding. The interconnect was then completed by mechanically finishing the end facets. To make this a completely automated DPAM process we plan on using a picosecond laser to finish off the end facets of the interconnect. The plastic fiber interconnect is then connected to a laser light source and a detector. This plastic optical fiber has a high delta n of 0.123 and can continue to transmit light effectively at tight bend radius below 5 mm. With current digital manufacturing equipment, these interconnects can be mass produced as well.

We will continue to explore our new optical interconnect by reviewing the numerical methods used to model the optical interconnect. We will look at the experimental methods used to fabricate the interconnects, results of interconnect characterization, and future work.

We have demonstrated that a plastic optical fiber can be produced by a composite additive manufacturing process called Direct Print Additive Manufacturing.

CHAPTER 2:

NUMERICAL METHODS

2.1 Numerical Characterization Using Geometric Optics

Optical fibers are typically broken into two groups, single-mode fibers with a comparatively small core which requires the wave model of light, and multimode fibers, whose core is large enough to be analyzed with a geometric ray-tracing model.[14]

Optical fibers work on the principle of total internal reflection of a radiation source through glass or plastic fiber inside of a cladding material. The critical angle for the total internal reflection follows:

$$\theta_{critical} = \sin^{-1}\frac{n_{cladding}}{n_{fiber}} \tag{2}$$

where $n_{cladding}$ is the refractive index for the cladding material and n_{fiber} is the refractive index for the fiber. For our fibers our critical angle is 69.33°. This is significantly higher than a standard fiber at about 28.2°.

The critical radius is the bend radius below which loss increases rapidly. For a multimode fiber the critical radius is given approximately by:

$$R_c = \frac{3n_1^2\lambda}{4\pi(n_1^2 - n_2^2)^{\frac{3}{2}}} \tag{3}$$

and with our materials and wavelength, we would expect a critical radius of about 1.35mm. At a bend radius below this we would expect losses to increase rapidly. This is another opportunity to vary the n values of the core and cladding and the wavelength to optimize the interconnect for different applications.

The path length that the radiation travels is determined by:

$$l = n_f L \sqrt{(n_f^2 - \sin^2 \theta_i)} \tag{4}$$

where L is the length of the fiber and Θ_i is the incident angle of the radiation. The difference in path length is important. The difference in path length that different fibers travel will cause issues in signal quality that will be discussed later in this section.

The number of reflections that the radiation will travel over a given distance is:

$$n_r = \frac{L \sin \theta_i}{D\left(n_f^2 - \sin^2 \theta_i\right)^{\frac{1}{2}} + / - 1} \tag{5}$$

where D is the diameter of the fiber. The larger the incident angle the more reflections that the radiation will have while traveling the length of the fiber, L.

The angle at which half of the radiation may enter the fiber is:

$$\sin \theta_{max} = \frac{1}{n_i}\left(n_f^2 - n_c^2\right)^{\frac{1}{2}} \tag{6}$$

and for our fiber our θ_{max} is equal to 36.39°. The total acceptance angle of the fiber to the radiation is:

$$\theta_a = 2\theta_{max} \tag{7}$$

which leads to an acceptance angle of 72.77°. Once again, this is significantly higher than a standard fiber.

The boundary of the two groups is determined by the structural parameter V:

$$V = \frac{2\pi\rho}{\lambda}\left(n_f^2 - n_c^2\right)^{\frac{1}{2}} \tag{8}$$

Light rays propagate via discreate paths through a fiber where each path is called a mode and corresponds to an angle of incidence. For our 77 μm fiber the V is 269. Different modes take different times to travel along the fiber. The total number of modes is defined by the numerical aperture which is given by:

$$NA = \left(n_f^2 - n_c^2\right)^{\frac{1}{2}} = n_0 \sin\left(\frac{\theta_a}{2}\right) \tag{9}$$

where n_0 = refractive index of the air. For our 77 μm fiber the NA is 0.5932. The larger the difference in refractive index, the higher the number of modes which can be guided through the fiber. With a step index fiber, the number of possible modes N_m is related by:

$$N_m = 0.5\left(\frac{\pi d NA}{\lambda}\right)^2 \tag{10}$$

where d is the diameter of the fiber and λ is the wavelength of the light used and, in our case, this is 532nm. At a core diameter of 77 μm with our PMMA Fiber and Optical Adhesive Cladding we are well into the multimode fiber range with over 36,000 modes. Our small diameter fiber at 9 μm is still a multimode fiber due to the large difference in the index of refraction and the low wavelength green laser that we are using for this program at 497 modes. The modes depend on

core diameter, the index of refraction for the cladding and wavelength. Evaluating the common parameters, we get the modes indicated in Table 1.

Table 1. How wavelength effects v-number and modes. Decreasing the fiber diameter decreases the number of modes. Decreasing the v-number by reducing the Δn will reduce the number of modes (and decrease the bending capability of the fiber).

Diameter (μm)	Wavelength (nm)	V-Number	# of Modes
77	532	269	36,377
	835	172	14,792
	1300	110	6,092
50	532	175	15,338
	835	111	6,160
	1300	71	2,520
9	532	31	497
	835	20	200
	1300	13	84
Glass - 9 μm (ref)	1300	0.84	1

Our optical cladding material comes standard in different refractive indexes between 1.315 and 1.700. With this large range of standard materials, we will be able to custom design the interconnect to different bend angles and transmission qualities. We can also utilize different core materials as PMMA has a refractive index of 1.492 and we can use urethane materials with lower n values than 1.492 with this core material. We can also explore other core materials with a higher refractive index like Cyclic Olefin Polymers (COP) at 1.53. By utilizing the DPAM process of FDM printing it is relatively easy to manufacture products with a range of core and cladding materials specifically for different applications.

Intermodal dispersion is an important topic in signal transmission in optical fibers. As different waves travel down a fiber at different angles they arrive at the end of the fiber at different times. This change in time can distort a signal. The change in time is indicated by:

$$\Delta t = \frac{L n_f}{c}\left(\frac{n_f}{n_c} - 1\right) \tag{11}$$

where L is the length of the fiber and C is the speed of light. An acceptable Δt is in the 4 ns second range and with small fibers where the Δn of the core and the cladding is small can be 4 ns over a kilometer with graded index fibers.[15] With this high Δn fiber, that can be bent significantly without transmission losses, the length of fiber that can be used in commercial application will be limited by this Δn to fiber lengths of less than 1 meter.

2.2 50 µm Multi-Mode Fiber Simulation

In an effort to better understand how fibers could be tightly routed through electronic devices, we need to understand when transmission breaks down and leaks out of the fiber, so we used ray tracing simulations to test ever tighter fiber bends until light began escaping our system.

Numerical simulations of the optical interconnect were performed using COMSOL with the Ray Tracing Module. A straight section of fiber with a 50 µm diameter PMMA core and our cladding material was simulated at 100% transmission. We then performed the simulation with increasingly tight bend radii from 1 m down to 2 mm. Transmission rates remain at 100% down to about 5 mm and decrease rapidly to 94% at 2 mm as shown in Figure 1.

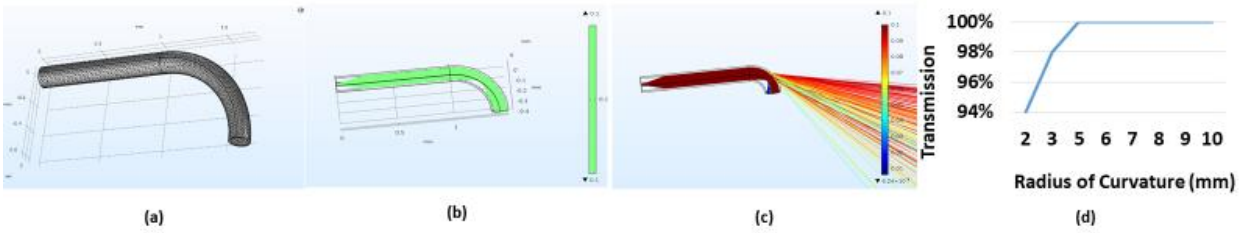

Figure 1. Numerical simulation of optical interconnect using COMSOL ray tracing. (a) 50-micron fiber was modeled, (b) Rays of light were injected into the fiber, (c) Decreasing bend radii were evaluated until a critical angle was reached and light escapes the fiber, and (d) Numerical simulation predicts high transmission levels at small angles of less than 3 to 5µm.

For industrial applications where, optical interconnects will be required to route through tight spaces, curved fibers will be required, and our simulations show that we should be able to successfully accommodate curves as tight at 2 to 5 mm without significant losses.

CHAPTER 3:

EXPERIMENTAL METHODS

A composite direct print additive manufacturing process (DPAM) micro-dispensing for pastes (conductive, resistive, insulating, etc.) and FDM for thermal deposition was used to create the first functioning additive manufactured 77 µm, 17 µm and 11 µm optical fibers. An example of a printed fiber and the printing process are shown in Fig 2.

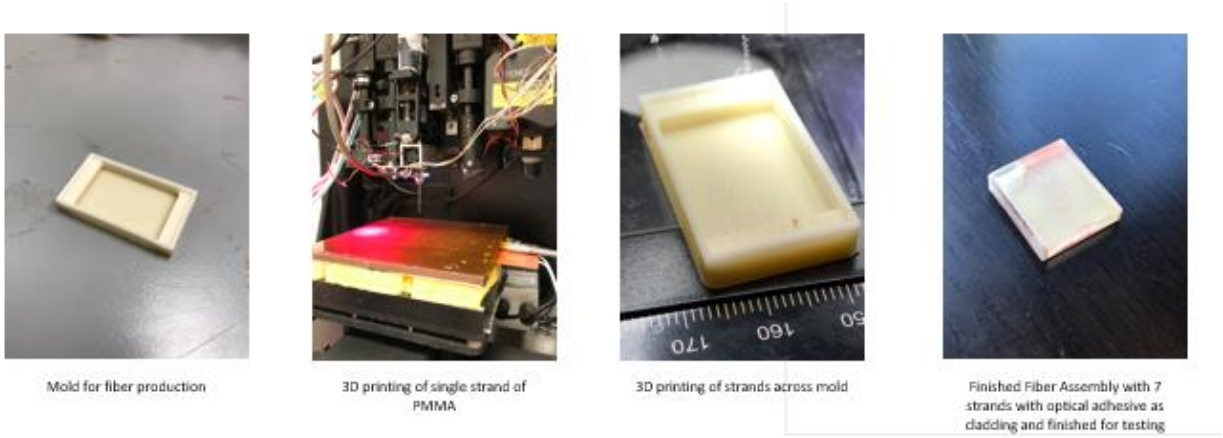

Figure 2. Fabrication of optical interconnects. (a) A guided channel base cladding, (b) FDM printing of a filament, (c) Multiple fiber printing, and (d) Finished optical assembly.

In the first air gap process (AGP), FDM printing was first used to create an acrylonitrile butadiene styrene (ABS) housing consisting of two ledges separated by a 26 mm air gap. The FDM process was again used to extrude a single filament of polymethyl methacrylate (PMMA) between ledges and across the air gap. A UV-curable optical adhesive blend of aliphatic urethane acrylate and acrylate monomer was dispensed and cured to form a cladding around the

PMMA core (NOA 1369). The end facets were then prepared using a cutting process and manually polished with abrasive media with increasingly smaller grain sizes to a surface roughness suitable for transmission testing.

A second surface printing process (SSP) was then developed to facilitate printing of three dimensional fibers. An ABS surface is created. The urethane cladding material is dispensed onto the base material and cured. The fiber is then FDM printed directly onto the cladding material. The cladding layer is completed with another layer of urethane on top of the FDM printed fiber and it is cured in place. Finally, the end facets are prepared so the device can be used. This second process will allow for complex fiber shapes to be printed to meet challenging routing applications.

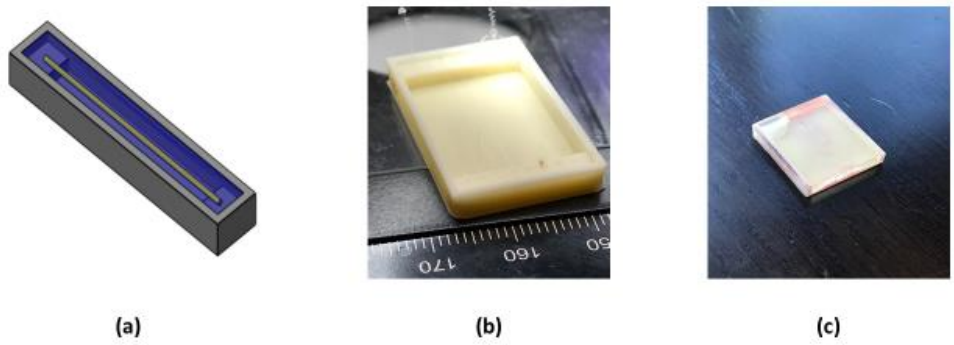

Figure 3. DPAM optical fiber design. (a) Concept of DPAM optical interconnect with an ABS housing, a PMMA core and an UV curing adhesive cladding, (b) Packed cores after printing, and (c) Finished 10 core interconnect with cladding and end facets prepared for testing.

3.1 Optical Interconnect Fabrication Details – 77 µm, Air Gap Process

Using an nScrypt digital manufacturing workstation, FDM printing was first used to create an acrylonitrile butadiene styrene (ABS) housing consisting of two ledges separated by a 26 mm air gap. The nScrypt machine used for this project has the ability to both FDM print and

dispense on the same machine. This particular machine has only one FDM print head which requires that the ABS filament is unloaded after the printing and another PMMA filament loaded for the next FDM step.

FDM was then used to extrude a single fiber of polymethyl methacrylate (PMMA)[14], with a refractive index of 1.492, from one standoff of the guided channel base cladding to the other standoff. PMMA has a high transmission rate of over 98% over 3mm with a single window at 550-650 nm wavelengths suitable for optic fiber communication at theoretically 55 dB/km at 570 nm.[14] A 50 µm zirconia nozzle was used for the FDM process. The nozzle was heated by a single cartridge heater to 260 C. The extruder speed was set to 0.1 mm/s and the nozzle traversed over the base at a speed of 20 mm/s. The temperature of the bed was set to 100C and remained there throughout the fabrication.

A micro-dispensed UV curable optical adhesive was applied into the housing to cover the fiber and acts as the cladding material. The material used was a Norland NOA 1369 low refractive index adhesive (1.369) at 2100 centipoises. The Norland NOA 1369 is a urethane based on 70-85% aliphatic urethane acrylate and 15-30% acrylate monomer. The modulus of elasticity of the adhesive is 73 MPA with a tensile strength of 7.8 MPA an elongation at failure of 52% and a hardness of 30 Shore D.

We cured the base cladding material with a UV light. The cladding material must be cured with UV light between 315 to 395 nm. Full cure requires 6 Joules/cm2. With our UV lamp at 395 nm and a power of 21,700 mW/cm^2 this will take about 5 minutes to achieve full cure. The adhesive exhibits oxygen inhibition when used as a coating and to overcome this the adhesive must be cured under an inert atmosphere such as nitrogen.

Light, which transmits through an optical waveguide passes through the ends of the optically transparent structure, are commonly referred to as end facets. These surfaces must exhibit specific characteristics to minimize the coupling losses and therefor the optical attenuation of the transmission path. It is required that the end facets have a low root mean square (RMS) surface roughness with smaller than a tenth of the transmitted wavelength ($\lambda/10$) to pressure wave front geometry. For the wavelength of 532 nm the RMS would need to be less than 53 nm. For this experiment, the end facets were prepared using a cutting process and then manually polished with abrasive media with increasingly smaller grain sizes.[6] Examination of the end facets under an optical microscope confirmed that we did not achieve the required surface roughness and would be a source of reduced transmission rates in testing.

3.2 Optical Interconnect Fabrication Details – 17 µm, Air Gap Process

Single mode optical fibers are required for some of today's more complex communications devices. Depending on the Δn of the cladding, typical single mode fibers are about 9 µm in diameter. To demonstrate a small fiber capability, we created a 17 µm fiber with the 10 µm nozzle. To fabricate this optical fiber, we followed the same AGP procedure that was described below with minor process condition changes. An example of a printed fiber is shown in Fig. 4(c), and the extruded fiber diameter was about 17 µm with a surface diameter variation of 1 to 2 µm. A Low-Pressure SEM process was used for the images in Fig. 12 so that they could be characterized without a conductive coating.

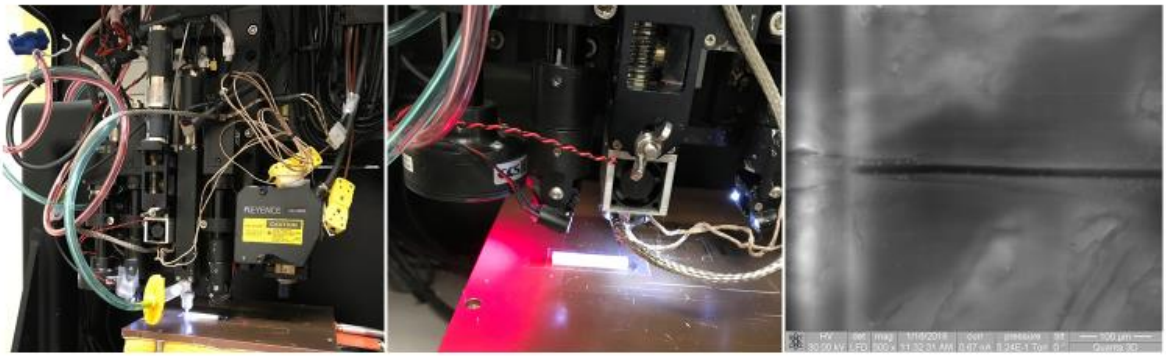

Figure 4. DPAM process to print an optical fiber onto a surface. (a) Urethane Cladding being dispensed onto an ABS form, (b) The PMMA core is printed onto the surface, and (c) The fiber embedded into a channel on the surface of the urethane cladding material.

3.3 Optical Interconnect Fabrication Details – 11 µm, Surface Printing Process

A useful fiber interconnect needs to be able to route through tight spaces, so our fiber needs to be able to bend in two or three dimensions. FDM printing a curved design, applying the urethane cladding material and then FDM printing the fiber directly on the fiber, and finally applying another layer of cladding would allow us to print complex shapes. The nScrypt DPAM equipment is perfectly suited to this as we can make a 3D ABS base and then use its laser guidance system to precisely follow the 3D shape with our dispensing and FDM printing.

This process was used successfully to print a 17 µm and an 11 µm fibers on the cladding material. The process is shown in Fig. 4 (a) and (b) and the fiber can be seen successfully embedded within the cladding material in Fig. 4 (c). The cladding material was dispensed automatically at a speed of 50 mm

CHAPTER 4:

RESULTS

4.1 77 µm AGP Fiber Characterization

To test the transmission capabilities of the new 3D printed optical fiber, a laser test station needed to be constructed. The basic principle is to shine a laser through the fiber and measure the power of the light before the fiber and after the fiber. The results of the transmission test are then compared to the transmission results from a commercial fiber of a similar type cut to the same length. The actual process is much more complicated and requires 11 different modules to accomplish this task.

4.1.1 Transmission Testing

The laser power is lowered through a filter and then reflected twice to get the beam aligned back to the sample. The laser light goes through a pellicle beam splitter and the light continues through a 40x objective lens that focuses the light on the optical fiber end facet. The light goes through the sample and is then focused again through a 20x objective lens into a spot on the power meter. The laser test work station was built to the design in Fig. 5 to test the light transmission capability of the new optical interconnect and the station that was built is shown in Figure 7.

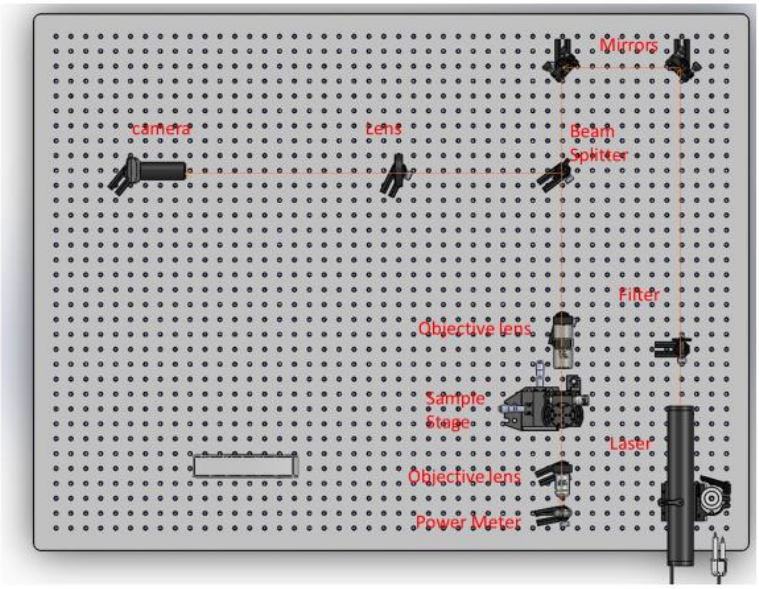

Figure 5. Laser test station. This setup uses a microscope objective to focus the laser and uses reflected light back through the beam splitter to see the front of the optical fiber, for aiming the laser at the center of the end facet of the fiber.

To align the laser to the optical fiber core, a reflected light microscope is built into the test system. The light was initially placed behind the fiber optic and used as a transmission light microscope, but not enough light could be collected to make this system work. More light is collected by a reflected light microscope, so a light source was placed in front of the sample optical fiber to provide the reflected light for the microscope and this provided more than enough light for the system.

Some of the light is reflected back through the objective lens and back to the pellicle beam splitter and about 4% of the light is reflected to the camera plane and is focused by the lens on the camera. Additionally, light is split off by the pellicle beam splitter opposite of the camera and must be stopped by a solid backstop. The focal length of the lenses and the position of the camera and samples will determine the magnification of the fiber end facet. 150 mm lenses were

used for the experiment. Figure 6 is an image from the integrated microscope that shows the cladding material with an optical fiber end facet which is shown in the right of the image. For the experiments, we must align the focused laser beam at the center of the optical fiber end facet.

At this stage we observed the poor quality of the end facets on the samples. A manual polishing process was used for the end facet preparation and it was obviously not good enough to achieve the 53 nm surface roughness that is required for optimal transmission. As we can see from Figure 6., the end of this fiber is damaged slightly. We have also introduced impurities into the cladding material and the immediate area between the cladding and the fiber. This end facet preparation no doubt negatively affected our transmission results.

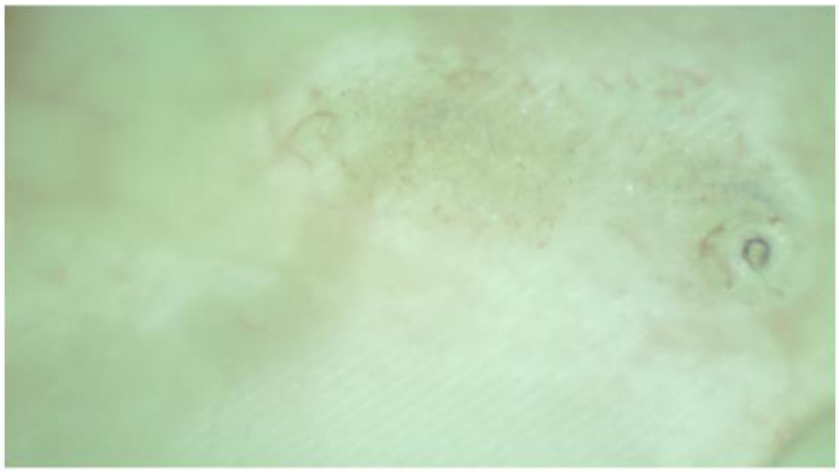

Figure 6. Alignment of the laser requires imaging by the hand-built microscope. The fiber core end facet is shown in the right side of the image. The laser beam is aligned so that the beam enters the center of the fiber.

The actual test station that was designed and built to test the transmission capability is indicated below in Figure 7. The green laser is the yellow box on the right of Figure 7(a). A 532nm laser was used for the work and it was filtered down to 1.32mW of power at the inlet of

the fiber. Using this setup on the fiber optic and using a commercial fiber as a reference, we were able to determine that the optical interconnect averaged a transmission rate of 45.6%.

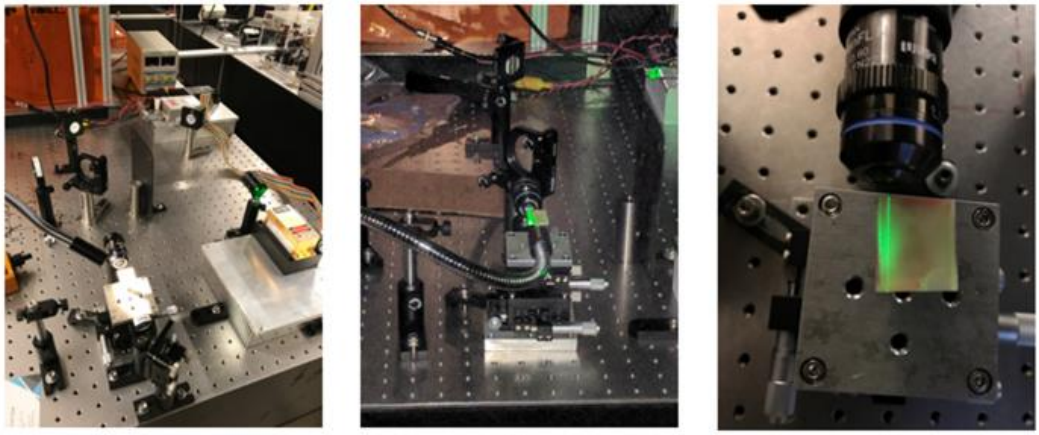

Figure 7. Laser evaluation of the digitally manufactured plastic optical fiber. (a) Actual laser test station setup, (b) The test sample in the rig with 532 nm wavelength laser is being used for the testing, and (c) Actual transmission of light through the fabricated plastic optical waveguide.

4.1.1 Scanning Electron Microscopy

One of the keys to a high fiber transmission is having very smooth walls on the fibers core. With fibers at less than 100 µm in diameter, the only reasonable way to evaluate the surface of the fiber was with a Scanning Electron Microscope (SEM). The SEM was an invaluable tool in characterizing the quality of the 3D printed fibers that were produced. The Hitachi model SU70 in the NREC was used for the work on the initial 77 µm fibers. Unclad 3D printed fibers made from a PMMA material were being evaluated. The fibers are a polymer material, so they are not conductive. To make the parts conductive they were sputter coated with a 14 nm layer of Gold/Palladium material on the surface using the Sputter Coater in the NREC.

Figure 8. Sample preparation for SEM. (a) Sputter of a gold/pallidum coating onto a PMMA plastic fiber so it is conductive, (b) Sample fiber after sputter coating, and (c) Actual SEM equipment used in imaging of fiber.

The first thing that was observed during the SEM work was that the fibers were very straight and smooth. The initial low magnification 30x scans showed a very straight fiber. Additional magnification to 200x confirmed that the 3D printed fibers are very straight and exceptionally smooth.

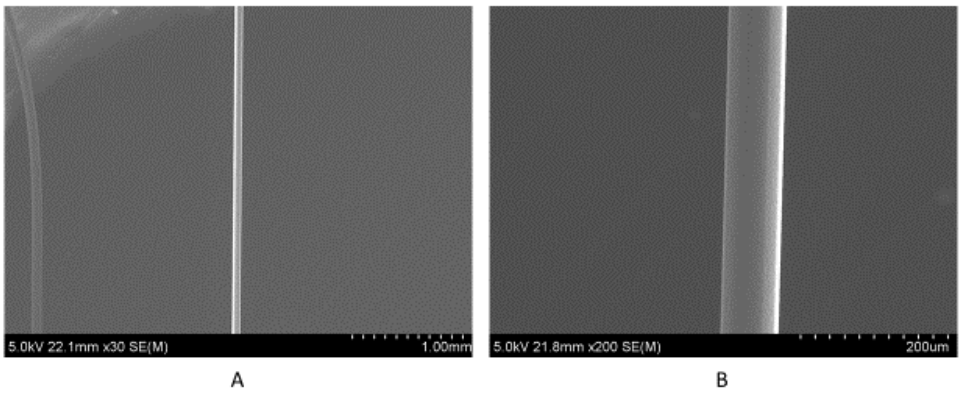

Figure 9. SEM images of smooth straight PMMA fibers that were produced using the DPAM process. (a) A 30x view of the fiber that indicates how straight the fiber has been extruded, (b) A 200x view of the fiber showing a very smooth surface.

Fiber optic communication happens because of total internal reflection of light inside of a fiber. One of the requirements for total internal reflection is a smooth fiber wall. For the target core diameter of 50 micron a surface variation of less than 1 μm for a high transmission optical fiber is needed.[16] The surface of the PMMA core is smooth with a maximum surface variation measured at about 425 nm. Multiple measurements across the fiber indicate that the average surface roughness is about 350 nm. This smooth surface is critical for total internal reflection to take place.

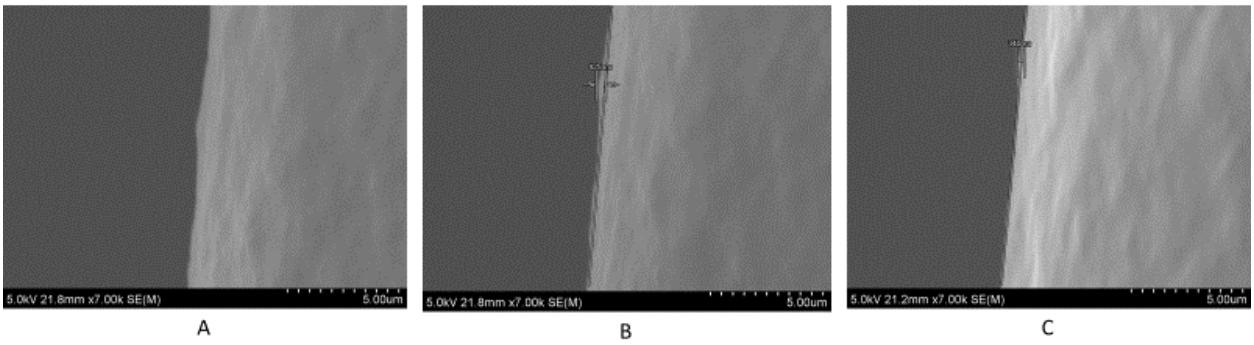

Figure 10. SEM results indicated a smooth optical core. (a) Average surface variation is very small, (b) The maximum surface variation measured is less than 425 nm., and (c) The average surface roughness is much closer to 340 nm.

A variation in diameter was seen in the SEM work and is illustrated in Figure 11. A 50 μm nozzle was used in the extrusion process. Due to swelling out of the extruder tip along with a slow initial traverse speed, the initial fiber diameter is about 87 μm. As the extruder traverse reaches a steady state the fiber reaches a nominal diameter of about 77 μm. This steady state is reached in about 1mm from the start of the extrusion.

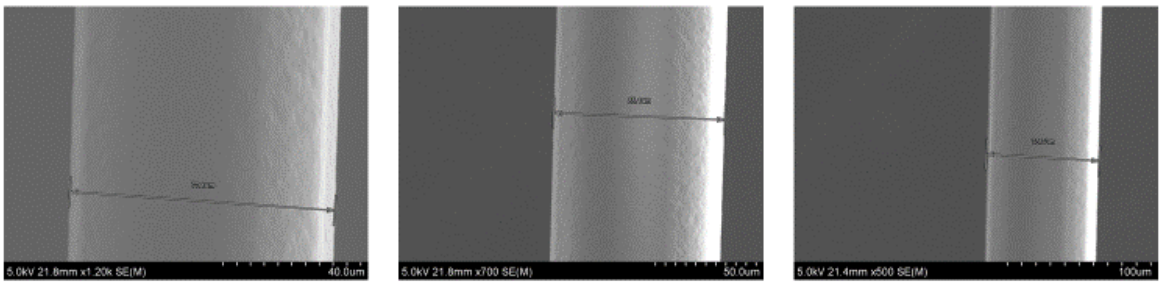

Figure 11. SEM image of the variation in diameter due non-uniform traverse speed across the extrusion span. (a) The nominal diameter of about 77 µm is achieved from a 50 µm nozzle, (b) The max diameter observed is about 85 µm at the start of the extrusion, and (c) Once the extruder reaches target traverse speed the thickness is down to the nominal 77 µm.

A uniform fiber diameter is critical to optical fiber performance and will be part of the engineering process of producing a good next generation prototype product.

4.2 17 µm AGP Fiber Characterization

To avoid having to coat our samples in a conductive material that might affect our surface roughness evaluation, we used low pressure SEM to evaluate the surface of the new smaller diameter fibers from the 10 µm tip. At this small diameter, the fiber diameter and surface roughness were higher than was observed at the larger diameter. The fibers swelled to about 17 µm out of the nozzle and the diameter varied about +/- 850 nm as can be seen in Fig. 12.

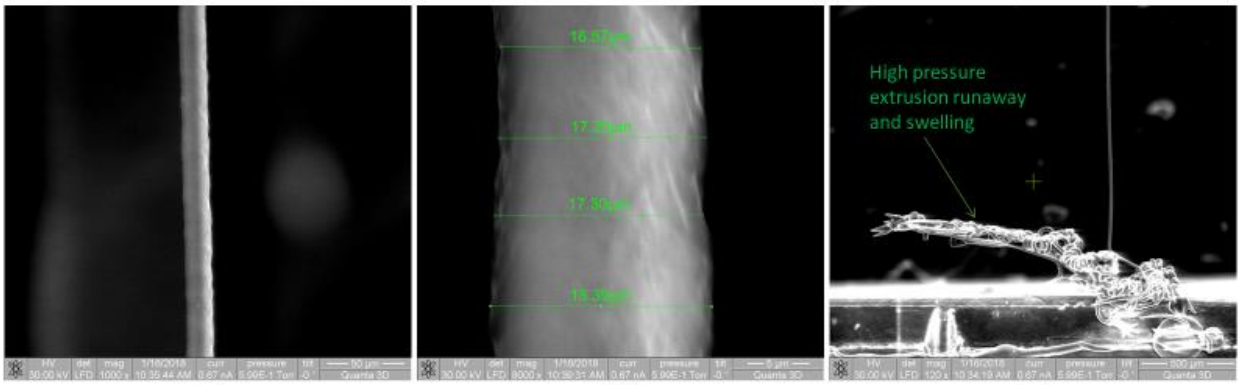

Figure 12. SEM evaluation of DPAM optical waveguide with a 9 µm FDM tip. (a) Typical surface of a DPAM manufactured PMMA fiber, (b) Surface roughness of between 1 and 2 µm is measured, and (c) Control of fiber during the FDM process is difficult with high pressure and temperatures required and leads to swelling and runaway extrusion.

4.3 11 µm SPP Fiber Characterization

Preliminary studies have been performed on a new DPAM process for printing small single mode size fibers on a (cladding) surface. This capability will enable AM printing of interconnects into complex and tightly packaged shapes, forming the basis for the proposed 3D optical interconnects. For this process the micro-dispensing head on the nScrypt 3Dn printer was used for adhesive cladding deposition; the cladding was UV cured under a nitrogen atmosphere. PMMA fibers were printed on the cladding surface using FDM and a 9 µm tip. The high temperature FDM tip softens the urethane cladding material, allowing the fiber to be routed through a trench made by the hot tip, or embedded within the cladding where the cladding material will reflow back over the fiber core. The quality of the fiber created in this process is very important. Embedded fibers appear to have an enlarged and rough surface. Fibers printed in a channel appear to be of small diameter with a very smooth surface finish that is appropriate for total internal reflection as seen in Fig. 13.

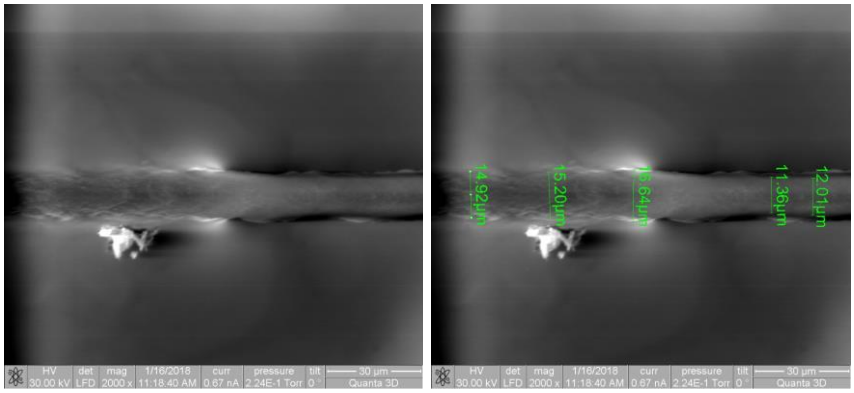

Figure 13. Single mode fiber printed on a cladding surface and embedded in a cladded surface. (a) FDM parameters can either imbedded in the fiber core in the cladding or in channel on the surface, and (b) Quality of fiber printed in a channel on the cladding appear much smoother and with a more uniform diameter.

CHAPTER 5:

CONCLUSION

5.1 Main Contributions

We have demonstrated that a plastic optical fiber can be produced by a composite additive manufacturing process called Direct Print Additive Manufacturing (DPAM).

A process was developed to produce a fiber across an Open-Air Gap (AGP). We used FDM printing and using a 50 µm nozzle we were able to fabricate 77 µm diameter fibers from a PMMA filament. The fibers were cladded with a UV curing urethane optical adhesive. Surface roughness measurements using SEM were less than 450 nm which are acceptable for transmission. The transmission of this fiber was determined to be about 46%.

Using this same AGP process, we were also able to fabricate a 17 µm fiber using a 10 µm nozzle. The surface roughness of these samples varied by 1.6 µm and would not be suitable for transmission. The difficulties in manufacturing at this small diameter have provided research opportunities that could lead to improved surface smoothness.

A process was also developed where the fiber is printed on a urethane optical cladding. This method of printing on a cladding material allows for three dimensional routings of additive manufactured optical fibers. Using a 10 µm nozzle on these fibers, we were able to print 17 µm fibers embedded into the cladding materials. The fibers embedded in the cladding had a variation in diameter of about 1.75 µm.

The fibers that were printed on the cladding material were about 11 µm in diameter with a variation of about 640 nm. The surface roughness was much improved for the fiber printed on the surface versus the same fiber embedded in the surface.

5.2 Future Work

Now that a plastic optical fiber has been produced by an additive manufacturing process, the process needs to be improved and then defined to repeatably produce a 50 µm multi-mode fiber and a 9 µm single mode fiber on a substrate in three dimensions with a high transmission rate.

The process should include the evaluation of different core and cladding materials and index of refractions to optimize different characteristics for different applications. High Δn materials for tight bend radius applications. Low Δn materials for low signal distortion for long distance applications. High n value core materials for high information density transmission applications.

Development of prototype products should be investigated. With industry partnership, we should create new inter-board interconnect devices that can be used to confirm design details in a production environment.

The DPAM process with its onboard laser could also be used to laser pole a PMMA / chromophore composite core material during the fabrications process. This poled core material would be ideal in an electro-optical modulator device. Once again this should be investigated along with an industrial partnership.

REFERENCES

1. Jun Su Lee, L.C., Carmelo Scarcella, Nicola Pavarelli, Sylvie Menezo, Stephane Bernab, Enrico Temporiti, and Peter O'Brien, *Meeting the Electrical, Optical, and Thermal Design Challenges of Photonic-Packaging.* IEEE JOURNAL OF SELECTED TOPICS IN QUANTUM ELECTRONICS, 2016. 22(6).
2. Nguyen, D.T., et al., *3D-Printed Transparent Glass.* Advanced Materials, 2017. **29**(26): p. 1701181-n/a.
3. Klein, J., et al., *Additive Manufacturing of Optically Transparent Glass.* 3D Printing and Additive Manufacturing, 2015. 2(3): p. 92-105.
4. Kotz, F., et al., *Three-dimensional printing of transparent fused silica glass.* Nature, 2017. 544(7650): p. 337-339.
5. Luo, J., H. Pan, and E.C. Kinzel, *Additive Manufacturing of Glass.* Journal of Manufacturing Science and Engineering, 2014. 136(6): p. 061024-061024-6.
6. Wolfer, T., et al., *Printing and preparation of integrated optical waveguides for optronic sensor networks.* Mechatronics, 2016. 34(Supplement C): p. 119-127.
7. Benner, A. *Optical Interconnect Opportunities in Supercomputers and High End Computing*. in *Optical Fiber Communication Conference*. 2012. Los Angeles, California: Optical Society of America.
8. Kuchta, D.M., et al., *64Gb/s Transmission over 57m MMF using an NRZ Modulated 850nm VCSEL*. 2014 Optical Fiber Communications Conference and Exhibition (Ofc), 2014.
9. Kobrinsky, M.J., et al., *On-Chip Optical Interconnects.* Intel Technology Journal, 2004. 8(2): p. 129-141.
10. Miller, D.A.B., *Optical interconnects to electronic chips.* Applied Optics, 2010. 49(25): p. F59-F70.
11. Keeler, G.A., et al., *The benefits of ultrashort optical pulses in optically interconnected systems.* IEEE Journal of Selected Topics in Quantum Electronics, 2003. 9(2): p. 477-485.
12. Kuan-Neng, C., et al., *Comparisons of conventional, 3-D, optical, and RF interconnects for on-chip clock distribution.* IEEE Transactions on Electron Devices, 2004. 51(2): p. 233-239.
13. Miller, D.A.B. and H.M. Ozaktas, *Limit to the Bit-Rate Capacity of Electrical Interconnects from the Aspect Ratio of the System Architecture.* Journal of Parallel and Distributed Computing, 1997. 41(1): p. 42-52.
14. P.V. Thorat, S.W., P.A. Thombre, *Plastic Optical Fiber*. International Journal of Engineering Research and Reviews, 2014. 2(4): p. 95-104.
15. Hecht, E., *Optics*. 2016, Pearson Education. p. 204-212.
16. Zhong, N., et al., *Effects of surface roughness on optical properties and sensitivity of fiber-optic evanescent wave sensors.* Applied Optics, 2013. 52(17): p. 3937-3945.